

Analysis of senescence-responsive stress fiber proteome reveals reorganization of stress fibers mediated by elongation factor eEF2 in HFF-1 cells

Shiyou Liu, Tsubasa S. Matsui, Na Kang, and Shinji Deguchi*

Division of Bioengineering, Graduate School of Engineering Science, Osaka University, Osaka 560-8531, Japan

ABSTRACT Stress fibers (SFs), which are actomyosin structures, reorganize in response to various cues to maintain cellular homeostasis. Currently, the protein components of SFs are only partially identified, limiting our understanding of their responses. Here we isolate SFs from human fibroblasts HFF-1 to determine with proteomic analysis the whole protein components and how they change with replicative senescence (RS), a state where cells decline in the ability to replicate after repeated divisions. We found that at least 135 proteins are associated with SFs, and 63 of them are up-regulated with RS, by which SFs become larger in size. Among them, we focused on eEF2 (eukaryotic translation elongation factor 2) as it exhibited on RS the most significant increase in abundance. We show that eEF2 is critical to the reorganization and stabilization of SFs in senescent fibroblasts. Our findings provide a novel molecular basis for SFs to be reinforced to resist cellular senescence.

Monitoring Editor

Kozo Kaibuchi
Nagoya University

Received: May 5, 2021

Revised: Oct 15, 2021

Accepted: Oct 20, 2021

INTRODUCTION

Stress fibers (SFs) are bundles of actin filaments expressed in mesenchymal cell types such as fibroblasts (Kreis and Birchmeier, 1980). SFs exhibit adaptive responses to changes in intracellular and extracellular cues by modulating assembly and disassembly (Tojkander *et al.*, 2012), which allows them to be involved in diverse cellular functions. Typical examples include the regulation of cell–substrate adhesion (Braga *et al.*, 1997; Livne and Geiger, 2016), cell migration (Hotulainen and Lappalainen, 2006), mechanotransduction (Chen

et al., 2004; Burridge and Wittchen, 2013; Hirata *et al.*, 2015; Wei *et al.*, 2020), morphological maintenance (Meng and Takeichi, 2009; Jalal *et al.*, 2019; Kang *et al.*, 2020), mechanical properties (Deguchi *et al.*, 2006; Kumar *et al.*, 2006), and avoidance of proinflammatory signaling and resulting cell homeostasis (Kaunas *et al.*, 2006; Chien, 2007; Kaunas and Deguchi, 2011).

Currently, the components that constitute SFs remain incompletely identified. In fact, only 20 proteins were listed in a recent review to be associated with the complex of SFs, which include cytoskeleton-binding proteins, adhesion proteins, and small GTPase-related enzymes (Tojkander *et al.*, 2012). Given, however, that more than 900 proteins have been reported based on proteomic analysis as constituting focal adhesions (FAs) connected to the termini of individual SFs to work cooperatively (Kuo *et al.*, 2011) and that SFs are engaged in such diverse biological functions under multifarious stimuli, it is likely that SFs actually consist of a much larger number of proteins. Thus, here we aim at comprehensively identifying the protein components inherent to SFs and how they change as cells undergo senescence, which is also a biological process that can intricately be linked to age-related diseases.

Replicative senescence (RS) is defined as a state in which normal somatic cells including fibroblasts decline in their ability to replicate *in vitro* after a long period of culture and repeated divisions (Goldstein, 1990; Muller, 2009). This cellular aging leads to

This article was published online ahead of print in MBoC in Press (<http://www.molbiolcell.org/cgi/doi/10.1091/mbc.E21-05-0229>) on October 27, 2021.

Conflict of interest: The authors declare that there is no conflict of interest.

Data availability statement: The data that support the findings of this study are available from the corresponding author on reasonable request.

*Address correspondence to: Shinji Deguchi (deguchi.shinji.es@osaka-u.ac.jp).

Abbreviations used: CALD1, caldesmon 1; eEF2, eukaryotic translation elongation factor 2; FA, focal adhesion; FC, fold change; FRAP, fluorescence recovery after photobleaching; FWHM, full width at half maximum; HFF, human foreskin fibroblast; MLC, nonmuscle myosin regulatory light chain; NMMIIa, nonmuscle myosin IIa; RS, replicative senescence; SA- β -gal, senescence-associated β -galactosidase; SF, stress fiber.

© 2022 Liu *et al.* This article is distributed by The American Society for Cell Biology under license from the author(s). Two months after publication it is available to the public under an Attribution–Noncommercial–Share Alike 4.0 International Creative Commons License (<https://creativecommons.org/licenses/by-nc-sa/4.0>). “ASCB®,” “The American Society for Cell Biology®,” and “Molecular Biology of the Cell®” are registered trademarks of The American Society for Cell Biology.

irreversible growth arrest accompanied by phenotypic changes such as flat cell morphology and increased senescence-associated β -galactosidase (SA- β -gal) activity. The close association with cell morphology suggests the involvement of SFs in RS. In fact, there are many reports describing their morphological change associated with RS, although the response seems to vary depending on the cell types (Hwang *et al.*, 2009). Meanwhile, RS-driven changes in the molecular components of SFs remain poorly understood except for actin, i.e., only their major constituent.

Here we investigate the effect of RS on SFs in human fibroblasts, typically used in RS-related studies. To this end, we isolate SFs from two different cell populations, young or aged, to compare the morphology and protein components between them with proteomic analysis. We found that SFs, identified here to consist of at least 135 different types of proteins, become thickened on RS with increased expression of 63 proteins including major protein nonmuscle myosin IIa (NMMIIa). Among them, we focused on a specific protein eEF2 (eukaryotic translation elongation factor 2) as it exhibited on the induced senescence the most significant increase in abundance in SFs while categorized as having diverse biological functions in the proteomic analysis. We then show that eEF2 is critical to the reorganization of SFs that are stabilized in senescent cells where proliferation and migration are both reduced. eEF2 is well characterized as an essential factor for promoting the mRNA translation by ribosomes (Choi *et al.*, 2018), but has rarely been reported with respect to the cytoskeleton. Thus, our findings provide a novel molecular basis for SFs to be reinforced to resist fibroblast senescence.

RESULTS

RS induces thicker SFs in fibroblasts

We induced RS to human foreskin fibroblasts HFF-1 by repeated passaging. The degree of the senescence was identified using several indicators, where the increases in SA- β -gal activity, p21 expression, and p53 expression are among the most common indicators. We found significant up-regulation of these indicators on the increased passage numbers, in which passage numbers 2, 10, and 33 (termed P2, P10, and P33, respectively) were selected as the target of the present analysis (Figure 1, A and B). P2, which has the relatively lowest degree of senescence, is regarded as a young control for the subsequent analyses. We compared the phenotypic characteristics, in which more senescent cells exhibited slower migration speed (Figure 1C), lower proliferation (Figure 1D), and increased cellular and nuclear areas (Supplemental Figure S1, A–C). Interestingly, senescent cells in suspended condition were also larger in the projected area than young cells, probably due to the increased size of their nuclei (Supplemental Figure S1, D and E). Focusing on individual SFs observed with phalloidin staining, they exhibited thicker morphology as RS proceeded, while there was no significant difference in the number per cell (Figure 2).

Validation of the isolation of SFs from cells

Motivated by the above finding that the morphology of SFs is altered on RS, we attempted to comprehensively identify the protein components of SFs that markedly change with RS. To this end, SFs were isolated from the rest of the cells for proteomic analysis (Figure 3A). Specifically, cells were treated with hypotonic shock to finally remove most of the cell bodies according to our and others' previously developed techniques (Kato *et al.*, 1998; Matsui *et al.*, 2011; Okamoto *et al.*, 2020), leaving ventral SFs physically attaching to the substrate. These SFs remained unchanged in appearance during the hypotonic shock treatment as observed with EGFP-actin transiently expressed in the cells (Supplemental Figure S2A). The ventral

SFs, now exposed to the solution, were next treated with a gentle detergent (0.05% Triton X-100) in a cytoskeleton stabilizing buffer to remove the underlying plasma membrane and its associated proteins as well as the nucleus. F-actin staining (Figure 3B) and immunofluorescence of anti- α -actinin-1, NMMIIa, and β -actin (Figure 3C) showed that these proteins remain associated along the length of the extracted SFs even after the cell bodies are removed. The RS-elicited increase in the thickness of individual SFs, observed in intact cells (Figure 2), was also detected even after they were extracted from the cells (Supplemental Figure S2, B and C); here, the thickness of SFs was defined as the full width at half maximum (FWHM) of the intensity profile. The presence of these proteins, in addition to non-muscle myosin regulatory light chain (MLC), was also confirmed in the extracted SFs with Western blotting performed by physically isolating them from the dish using a rubber scraper (Figure 3D). Meanwhile, other proteins that are not typically associated with SFs—specifically fascin, vinculin, tubulin, and GAPDH—were almost absent in the isolated SF lysates and instead were detected in the cell body lysates. Importantly, fascin, an F-actin cross-linking protein essential for the formation of filopodia and lamellipodia but not SFs, was present only in the cell body lysates. These results support that the subcellular materials that inherently constitute SFs were isolated from the rest of the cells while keeping apparent morphology and compositions.

Proteomic analysis reveals RS-induced up-regulation of eEF2 within SFs

We performed shotgun proteomic analysis on the isolated SFs to evaluate how they change in composition between the two extremely different passage numbers P2 and P33 with three independent experiments (Figure 3A). We reproducibly identified 135 proteins out of 362 detected proteins in the isolated SFs (Supplemental Table S1): in this table, the proteins are categorized to three groups in accordance with the magnitude of the fold change (FC) in the ratio of expression level of each protein at P33 to that at P2 as $FC \geq 2$, $2 > FC > 0.5$, or $0.5 \geq FC$, i.e., representing that, in response to RS, the protein is up-regulated, unchanged, or down-regulated, respectively. The number of the identified proteins, 135, is much larger than that previously listed as the components of SFs, 20 (Tojkander *et al.*, 2012), thus potentially allowing us to detect novel proteins that were not known to be associated with SFs. Of the 20 proteins, on the other hand, only 13 were identified in our study (specifically, MYH9, PALLD, SEPT2, filamin A (FLNA), TPM4, caldesmon 1 (CALD1), PDLIM7, CSR1, ACTN1, VASP, CNN2, ZYX, and TAGLN), but the rest were not detected for some reason, e.g., the specific cell types used, protein sensitivity to different experimental treatments, and/or the small amount of protein association to SFs.

Focusing on proteins in the volcano plot with a p value of < 0.05 in Student's t test and an FC value of ≥ 2 or ≤ 0.5 , we identified 11 proteins (PRDX2, PRDX1, ANXA2, S100A11, AP2A1, β -tropomyosin (TPM2), eEF2, VASP, CSR2, FLNA, and CALD1) for $FC \geq 2$ group and 7 proteins (RPL30, HNRPA1, THY1, RAB1, RPL18, RPLP2, and CANX) for $FC \leq 0.5$ group (Figure 4A). Regarding all 135 proteins, we performed a literature/database review (particularly using GeneCards; Weizmann Institute of Science) to identify those that have been well documented to be related to the cytoskeleton. Consequently, 30 are listed to be associated with actin filaments and/or SFs, and 9 are with intermediate filaments and/or microtubules (Supplemental Figure S3). The 135 proteins are also categorized in accordance with the known biological processes using Scaffold software (Proteome Software) into one or more of the following eight groups (Figure 4B): "Biological Regulation" (37), "Cellular Process"

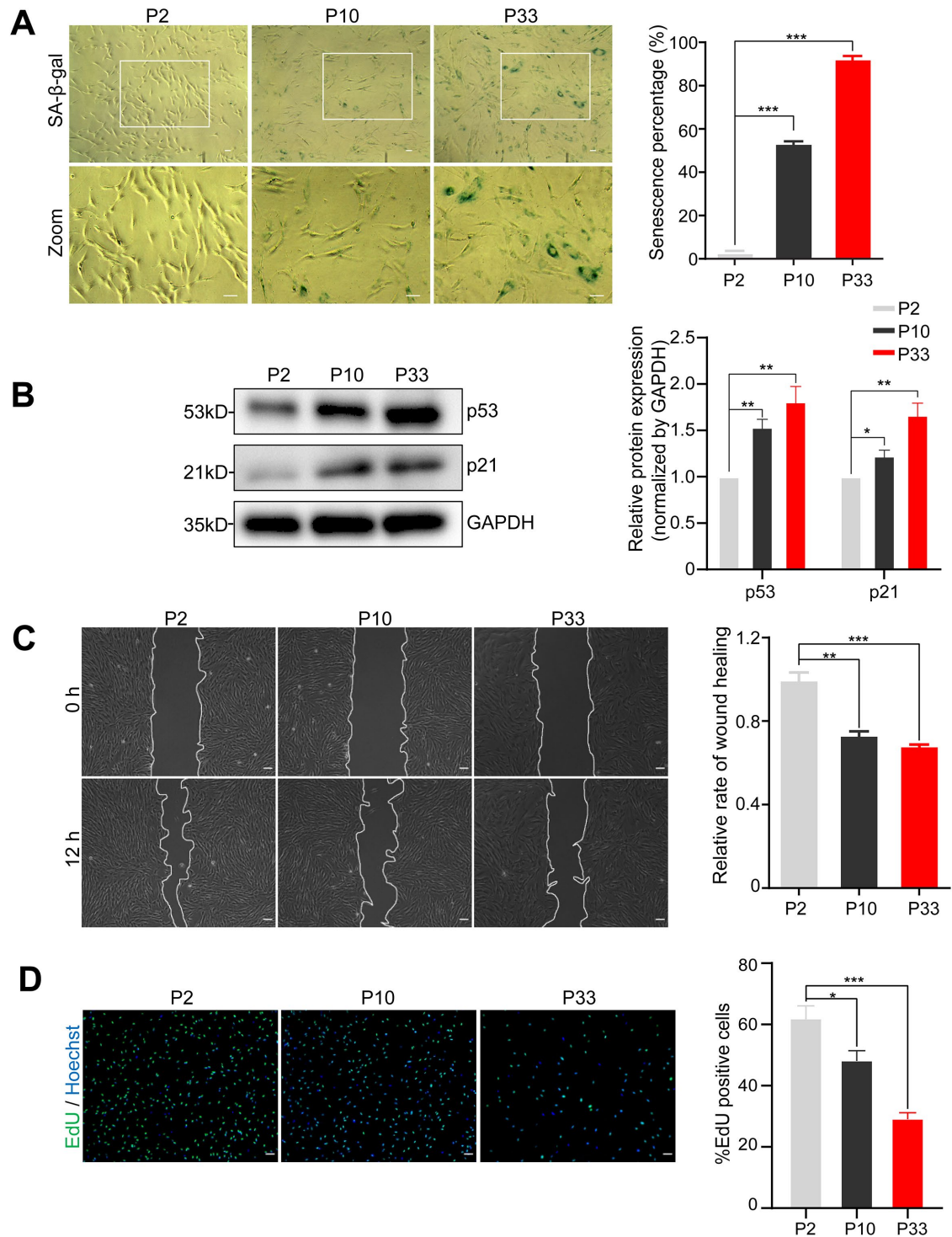


FIGURE 1: Induction of RS on HFF-1 cells. (A) The extent of senescence in cells passaged 2, 10, and 33 times (shown as P2, P10, and P30, respectively) was evaluated 24 h after SA-β-gal staining and quantified (P2, $n = 405$ cells; P10, $n = 363$ cells; and P33, $n = 327$ cells; $N = 3$ independent experiments for each group). (B) Protein expression levels of p53 and p21 were analyzed with Western blotting and quantified ($N = 3$ independent experiments; normalized by GAPDH). (C) Wound healing assay performed for 12 h and its quantification. White curves in the images represent the front border of the migrating cells. The scratched area in between the white line was used to calculate the healing rate ($N = 3$ independent experiments). (D) EdU proliferation assay performed for 36 h and its quantification (P2, $n = 803$ cells; P10, $n = 672$ cells; and P33, $n = 351$ cells; $N = 3$ independent experiments for each group). Scale, 100 μm.

(75), "Developmental Process" (27), "Establishment of Localization" (24), "Immune System Process" (14), "Metabolic Process" (56), "Multicellular Organismal Process" (25), and "Response to Stimu-

lus" (21), in which the figure in parentheses represents the number of proteins included in the respective group. As RS is related to diverse biological activities such as development, metabolism, stress,

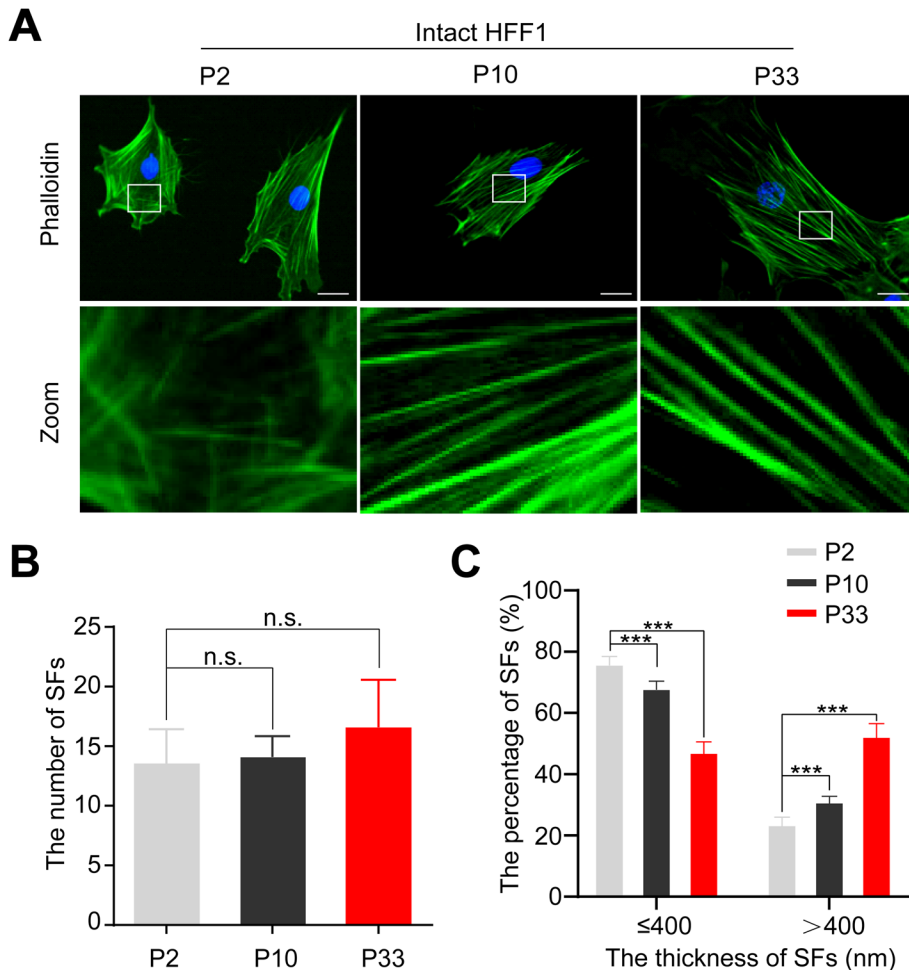


FIGURE 2: RS induces thick SFs. (A) Actin filaments (phalloidin, green) and nuclei (Hoechst, blue) in HFF-1 cells at different senescence levels of P2, P10, and P33. The bottom panel shows high magnification of the area outlined by the white box in the top image. (B, C) The number of individual SFs (B) and the ratio of the number of individual SFs with a thickness of ≤ 400 nm or of >400 nm to the whole population (C) at P2 ($n = 20$ cells, 291 SFs), P10 ($n = 20$ cells, 297 SFs), and P33 ($n = 20$ cells, 332 SFs) from $N = 3$ independent experiments. Scale, 100 μm .

and cancer progression (van Deursen, 2014), it may not be surprising that the 135 SF-associated proteins range over such various categories.

Next, we sought for proteins that are implicated in all of the above eight biological processes. Consequently, we obtained the following four proteins: THBS1, CD44, ITGB1, and eEF2 (Figure 4B; Supplemental Table S2). Among them, eEF2 was the only significantly up-regulated protein with an FC of 5.72. Taken together, we isolated SFs from fibroblasts with or without RS and found that $\sim 71\%$ (96 out of 135) of the associated proteins had not been well characterized as the constituents of SFs (Supplemental Figure S3). In view of the high sensitivity to RS, relevance to diverse biological processes and lack in understanding of its involvement in SFs, hereafter we focus on the specific protein eEF2.

Colocalization of endogenous eEF2 with SFs becomes prominent on RS

Consistent with the above proteomic analysis, Western blotting on the isolated SFs showed that the expression in eEF2, known as one of the elongation factors, increases with the progress in RS (Figure 5, A and B). Representative proteins associated with SFs, i.e.,

NMMIIa, α -actinin, and β -actin, showed a similar tendency; as a negative control, here we selected a protein with no significant change in the proteomic analysis, eEF1A1, and indeed Western blotting showed no significant change in the expression of eEF1A1. In a separate analysis, we found that SFs isolated from senescent cells at P33 contain a higher accumulation of eEF2 than young cells at P2, suggesting an increased association of eEF2 with SFs during RS (Supplemental Figure S4). Anti-eEF2 immunofluorescence was also performed to investigate the localization of endogenous eEF2 in HFF-1. For young cells at P2, eEF2 is mainly localized in the cytoplasm but is also weakly detected along the length of SFs (Figure 5C). At P33, the colocalization becomes prominent as eEF2 shows fibrous patterns like those of SFs. The extent of the accumulation to SFs was quantified by taking the ratio of eEF2 intensity at P10 or P33 to that at P2, showing that it significantly rises as the senescence proceeds to be more than twice at P33 compared with P2 (Figure 5D). We observed a similar RS-induced eEF2 up-regulation at the whole cell level as well with Western blotting, which occurs along with an increased expression in NMMIIa, α -actinin-1, and β -actin (Figure 5, E and F). Here, the degree of the increase in eEF2 expression was lower in the whole cell level (Figure 5, E and F) compared with that in the isolated SFs (Figure 5, A and B) because all eEF2 molecules are not necessarily bound to SFs (Supplemental Figure S4).

eEF2 is critical to the RS-induced enhancement of SFs

To explore if eEF2 has a role in the RS-mediated enlargement of SFs, or if the increased expression of eEF2 is just a consequence of the enlargement of SFs, we silenced eEF2 using siRNA in HFF-1 at P33 and observed the response of SFs. The immunofluorescence showed that the abundance of endogenous eEF2 is decreased by the silencing, and consequently SFs particularly located in the cytoplasm are significantly weakened or disappear (Figure 6A). The remaining SFs under eEF2 silencing were significantly decreased in thickness (Figure 6B). Western blotting showed that the expression of NMMIIa and α -actinin-1 was significantly down-regulated on eEF2 silencing, but that of β -actin was not changed significantly (Figure 6, C and D). The similar tendency was observed in the SFs isolated from cells with eEF2 silencing (Supplemental Figure S5, A and B).

We further analyzed the effect of overexpressing eEF2 in young HFF-1 at P2 and found that more visible, thicker SFs appear on the overexpression compared with control (Figure 6, E and F). The consistent tendency was observed with Western blotting in which the expression of NMMIIa and α -actinin-1 is significantly up-regulated on eEF2 overexpression not only in intact cells (Figure 6, G and H) but also in isolated SFs (Supplemental Figure S5, C and D).

We next analyzed the effect of eEF2 on the stability of SFs by performing fluorescence recovery after photobleaching (FRAP)

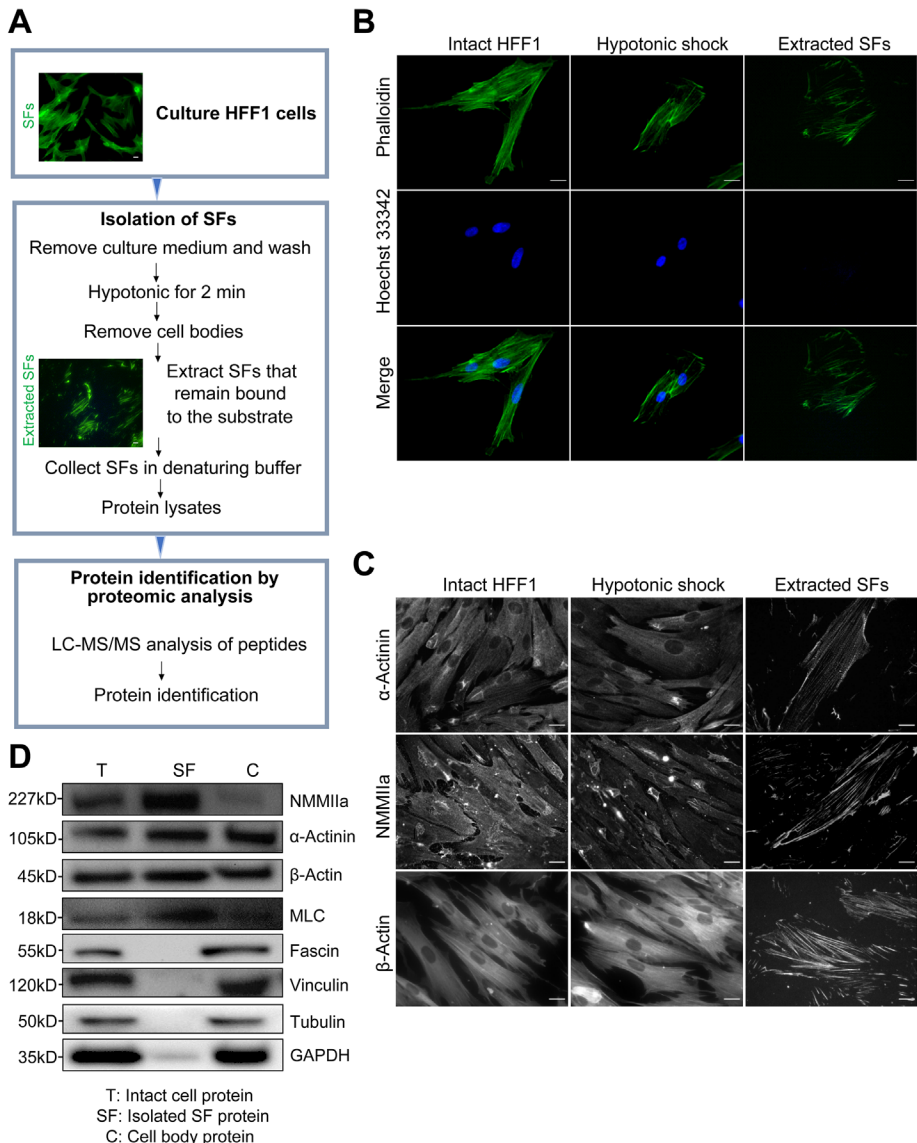


FIGURE 3: Isolation of SFs. (A) Flow chart for the isolation of SFs from HFF-1 cells and the component identification by proteomic analysis. Intact HFF-1 cells (top panel) and isolated SFs (middle panel) were stained with phalloidin. (B, C) Actin filaments (phalloidin) and nuclei (Hoechst) (B) and immunofluorescence of α -actinin-1, NMMIIa, and β -actin (C) in intact HFF-1 cells at P2 (left); those subjected to hypotonic shock (middle); and those after the extraction procedure (right). Note that the nuclei are finally removed and thus are absent in the extracted SF samples. (D) Immunoblot of the proteins contained in the total cell lysates (T), isolated SF lysates (SF), and cell body lysates (C). Scale, 20 μ m.

experiments. EGFP-tagged MLC was used as a marker of SFs in the senescent HFF-1 at P33 with or without eEF2 silencing given that previous studies (Watanabe *et al.*, 2007; Matsui and Deguchi, 2019; Horvath *et al.*, 2020; Huang *et al.*, 2021; Saito *et al.*, 2021) have shown that the dynamics of MLC—a major regulator of actin–myosin interaction—is closely associated with the stability of SFs. The fluorescence of EGFP-MLC recovered faster with the silencing, suggesting that the depletion of eEF2 destabilizes the senescent SFs (Figure 7, A and B). This tendency was quantified by analyzing the mobile fraction of the fluorescence, which measures the instability of SFs and was indeed found to significantly increase with eEF2 silencing (Figure 7C). Together, these results suggest that eEF2 mediates and stabilizes the RS-induced enhancement of SFs.

(Tojkander *et al.*, 2012). This situation for SFs is distinct from that for FAs as a comprehensive proteomic analysis was previously performed on isolated FAs to eventually identify that 905 proteins are associated with FAs, while 459 of them change in abundance on myosin II inhibition (Kuo *et al.*, 2011). The isolation of FAs was achieved with hypotonic shock and subsequent strong trituration on HFF-1 fibroblasts while minimizing contamination by SFs. In the present study, we took a similar approach by isolating SFs with hypotonic shock and more gentle fluid shearing forces on the same fibroblast cell line. Our isolation method using a cytoskeleton-stabilizing buffer has been extensively validated in many aspects including the maintained helical microstructures, associated proteins, and contractile function (Matsui *et al.*, 2011; Deguchi *et al.*, 2012;

DISCUSSION

Human fibroblasts have been used for decades as a model for understanding the basis of cellular senescence (Goldstein, 1990). Particularly, RS of fibroblasts is known to capture the features of cellular senescence in tissues (Hayflick, 1965; Cristofalo *et al.*, 2004). Indeed, we observed increased SA- β -gal positive cells and elevated expression of p53 and p21 in human fibroblasts HFF-1, which are recognized as reliable markers of cellular senescence (Levine and Oren, 2009; McHugh and Gil, 2018). Using this cell line, we demonstrated that proliferation, migration, and enlargement of cellular and nuclear areas are all altered on RS in a manner typical of the actual senescence.

Along with these responses, interestingly, a significant thickening of individual SFs is induced in senescent cells. It remains, however, controversial whether senescence leads to thicker or thinner SFs (Chen *et al.*, 2000; Nishio and Inoue, 2005), despite their inherent connection to cell morphology and migration (Hotulainen and Lappalainen, 2006; Meng and Takeichi, 2009; Lin *et al.*, 2017; Kang *et al.*, 2020; Kang *et al.*, 2021). As fibroblasts in tissues are subjected to various environmental cues including hormone signaling and wound remodeling, these individual differences are likely to be caused by complicated mechanisms (Hwang *et al.*, 2009). Nevertheless, to gain better insight into the mechanisms, not only just observing the morphology but also specifying the molecular identity intrinsic to SFs at different senescence stages must be indispensable. We therefore attempted to physically isolate individual SFs from HFF-1 and explore their protein reorganization in response to RS. We then found that there is indeed a significant compositional change on RS.

To our knowledge, the present study is the first that comprehensively elucidates the proteome of SFs and furthermore how it changes on cellular senescence. Despite increasing research on SFs, knowledge of their components has been highly limited

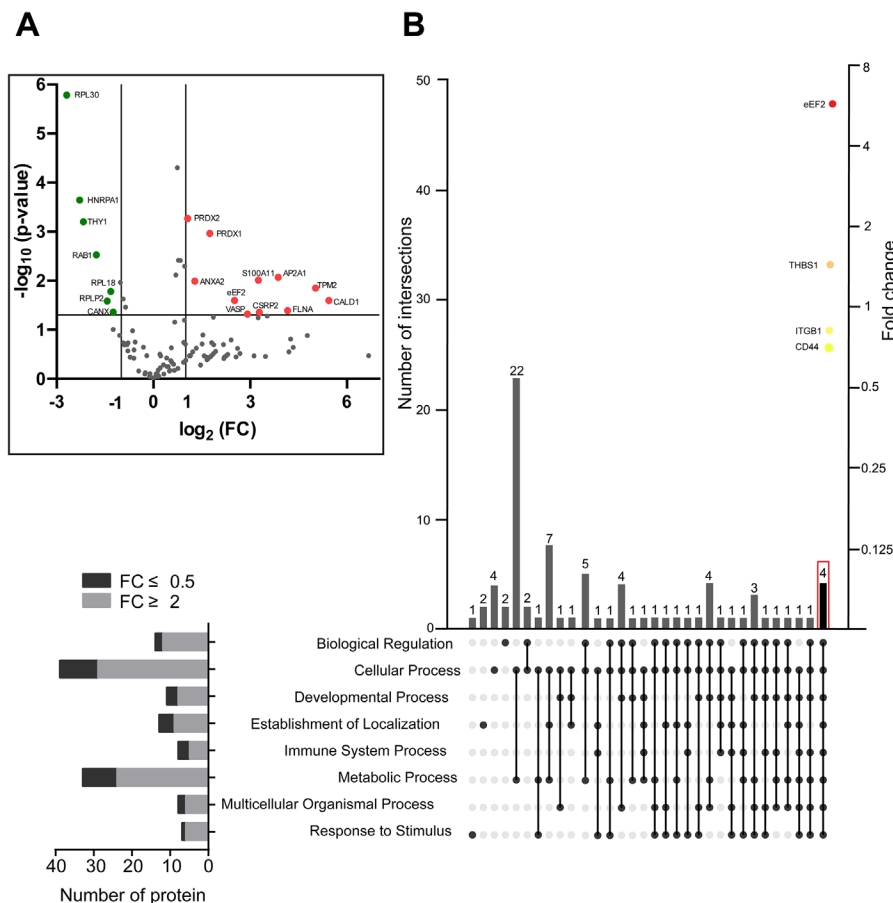


FIGURE 4: Proteomic analysis of isolated SFs reveals significant increase in eEF2 expression on RS. (A) Volcano plot shows differentially expressed proteins with a FC of ≥ 2 or ≤ 0.5 between young and senescent cells. The horizontal and vertical lines represent $p = 0.05$ and $\text{FC} = 0.5$ and 2, respectively. (B) In total 135 proteins were identified to be associated with the isolated SFs (Supplemental Table S1). Among them, 39 were already commonly known to be associated with the cytoskeleton according to the GeneCards database (Supplemental Figure S3), and therefore the rest (96 proteins) were focused on here and categorized according to the known eight biological processes (described below in the diagram) using the Scaffold software. Of these, eEF2 is one of the four proteins involved in all the eight processes and shows the most significant increase among the four in the amount of the association to SFs in response to RS.

Okamoto *et al.*, 2020). We then succeeded in specifying at least 135 proteins as the components of SFs, and among them 63 and 11 are up-regulated and down-regulated on RS, respectively (Supplemental Table S1). These large numbers seem to reflect the variety of biological processes to which SFs are potentially related and thus given the lack of relevant proteome information, the data obtained here will be of value in further studies.

Of the 135 proteins, RS increases $\sim 47\%$ ($\approx 63/135 \times 100$) in expression abundance, while only less than 8% ($\approx 11/135 \times 100$) is decreased, suggesting that SFs are reinforced to resist cellular senescence. Approximately one-third of the up-regulated ones ($19/63 \approx 0.30$) belong to the actin cytoskeletal component that includes CALD1, β -tropomyosin (TPM2), and FLNA, which are particularly enriched in the aged SFs (Supplemental Table S1). The increased abundance of proteins known as SF-associated components (Supplemental Figure S3) seems to be consistent with our observations that SFs become large with RS and previous reports that β -tropomyosin is essential for the maintenance of SFs (Tojkander *et al.*, 2011, 2012). On the other hand, we expected this first comprehensive analysis on

the composition of SFs might include undiscovered proteins that alter the size of individual SFs. We then focused on elongation factor eEF2 as it exhibited the most significant up-regulation with RS among the detected proteome that covers diverse biological functions (eEF2, CD44, ITGB1, and THBS1; Figure 4B).

We found that eEF2 is condensed in SFs of cells undergoing RS (Figure 5). Moreover, eEF2 was found to be critical to the RS-driven thickening (Figure 6) and maturation of SFs (Figure 7). As the tendency of the major SF-associated protein expression in eEF2 overexpression and silencing was consistent between the whole cells and the isolated SFs (Figure 6 and Supplemental Figure S5), our results seem to imply that eEF2 may directly contribute to the thickening of SFs. There is a previous report in which another elongation factor eEF1 was shown, surprisingly, to be involved in bundling the actin filaments to regulate the morphology of yeast cells independent of the mRNA translation function (Gross and Kinzy, 2005; Hamey and Wilkins, 2018). It remains unknown if eEF2 also possesses such similar actin bundling functions in fibroblasts in addition to its well-characterized translation activity; but, if this holds true, our results may reflect that SFs are stabilized in senescent human fibroblasts not only just by increasing the abundance of conventional actin bundling proteins of NMMIIa and α -actinin-1 but also by up-regulating eEF2 as an additional actin cross-linker to further mature the macromolecular structure of SFs while modulating the independent mRNA translation function. Determining the availability of eEF2 in actin bundling will be the subject of future investigation. On the other hand, given the increased abundance of the typical SF-associated proteins such as

NMMIIa, α -actinin-1, and β -tropomyosin (Supplemental Figure S3 and Supplemental Table S1), the possibility that the role of eEF2 here to promote the expression of those major SF components has not yet been ruled out.

In recent studies, eEF2 has increasingly been implicated in neurosynaptic plasticity (Verpelli *et al.*, 2010), NF- κ B-associated innate immune response network (Bianco *et al.*, 2019), and tumor progression as an oncogene (Oji *et al.*, 2014; Sun *et al.*, 2015; Rong *et al.*, 2020). While the relevance of eEF2 to the cytoskeleton remains poorly elucidated, these discoveries may suggest its role in cytoskeletal regulation. In fact, close interactions between the actin cytoskeleton and the protein translational machineries have been suggested (Kim and Coulombe, 2010; Silva *et al.*, 2016; Simpson *et al.*, 2020). Given this situation, our findings shed a new light on the molecular basis of the actin-based structure SFs and how their proteome is modulated to cope with senescence progression.

MATERIALS AND METHODS

[Request a protocol](#) through *Bio-protocol*.

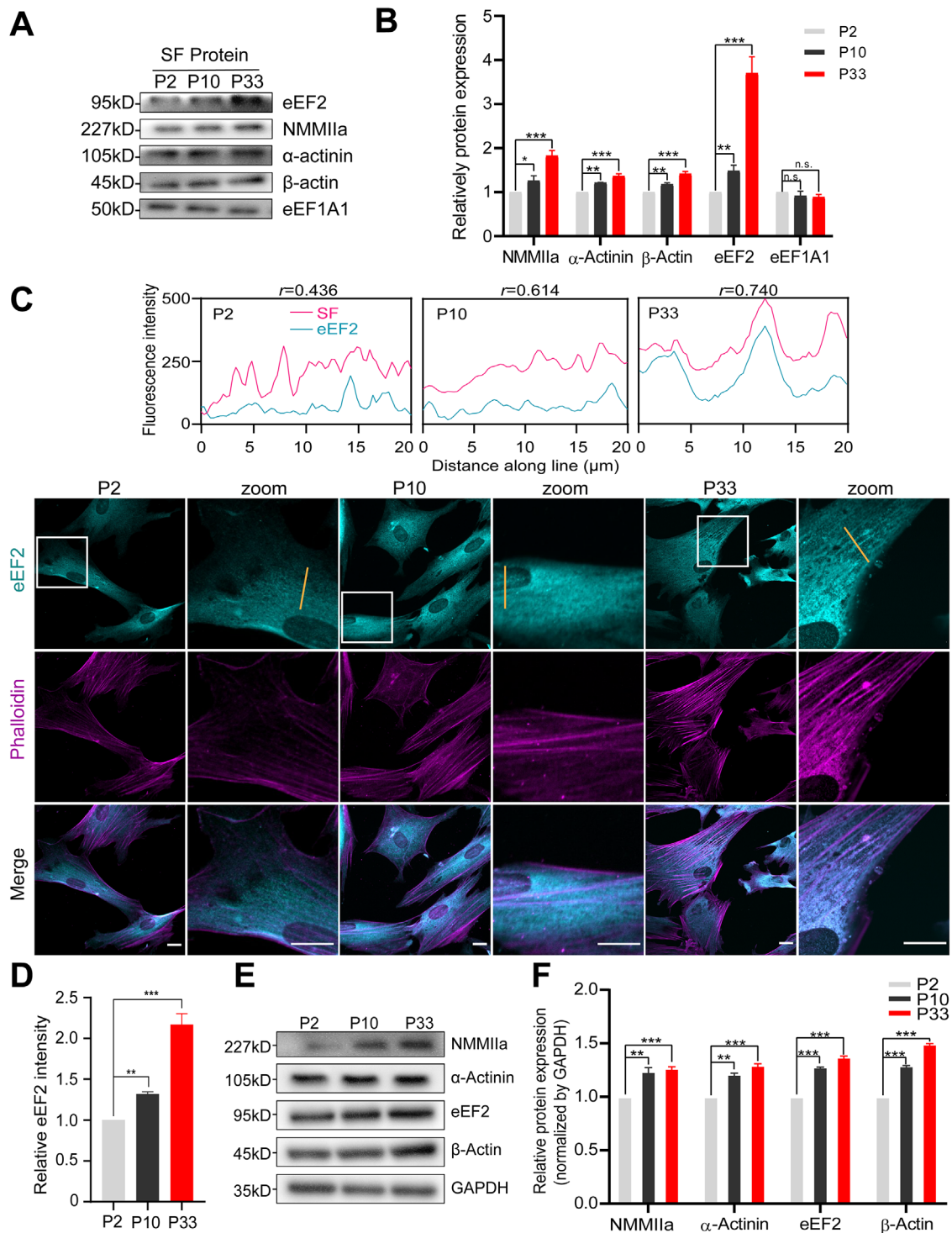


FIGURE 5: RS enhances localization of eEF2 to SFs. (A, B) Western blot shows increased expression of eEF2, NMMIIa, α -actinin, and β -actin in isolated SFs on RS ($N = 3$ independent experiments). (C) Top panel: intensity distributions along the length of the orange lines in the below images show increased localization of eEF2 on SFs (phalloidin) with a Pearson's coefficient r of up to 0.740 at P33. Bottom panel: immunofluorescence of eEF2 to observe the endogenous localization at the different senescence levels. The areas with the white rectangles are magnified on the right in each case. Scale, 20 μ m. (D) Quantification of the ratio of eEF2 fluorescence intensity at P10 ($n = 10$ cells) or P33 ($n = 10$ cells) to that at P2 ($n = 10$ cells). (E, F) Western blot shows increased expression in eEF2 and major SF proteins in intact cells in response to RS ($N = 3$ independent experiments; normalized by GAPDH).

Cell culture and transfection

Human foreskin fibroblasts HFF-1 (ATCC) were cultured with DMEM (high glucose) including L-glutamine and phenol red (Wako) supple-

mented with 15% fetal bovine serum (Sigma-Aldrich) and 1% penicillin-streptomycin solution (Wako) in a 5% CO_2 incubator at 37°C. Cells were transfected with plasmids or siRNAs using Lipofectamine

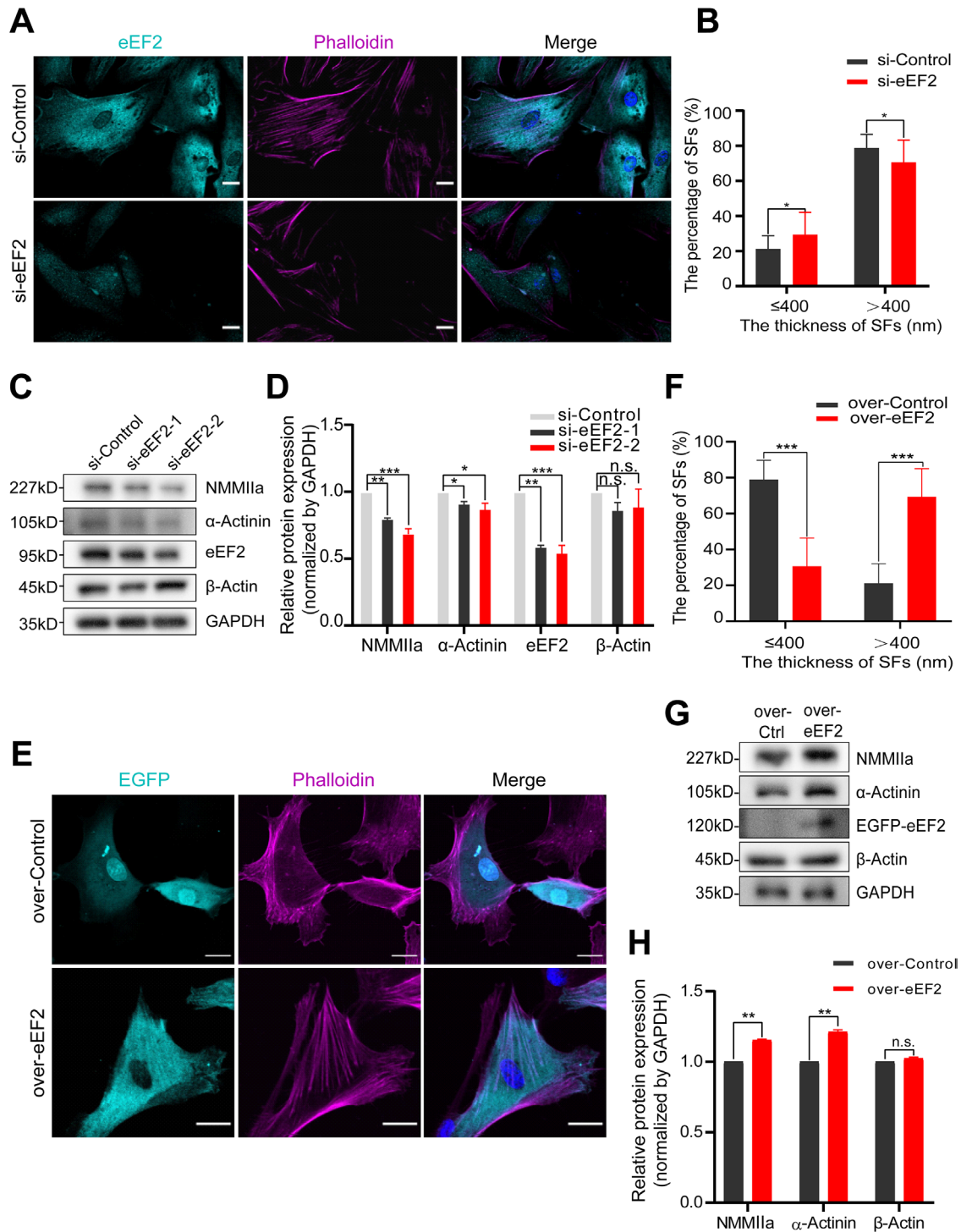


FIGURE 6: eEF2 is critical to SFs. (A) Immunofluorescence of eEF2 and F-actin staining in cells at P33 expressing siRNA for control or for eEF2. Scale, 20 μ m. (B) Quantification shows that the thickness of individual SFs in the cytoplasm is decreased on the silencing of eEF2 (si-Control, $n = 219$ SFs, 16 cells; si-eEF2, $n = 116$ SFs, 10 cells; from $N = 3$ independent experiments). (C, D) Western blot shows decreased expression in NMMIIa and α -actinin-1 on the silencing of eEF2 (where two types of siRNAs were used), but the concomitant change in β -actin is not significant ($N = 3$ independent experiments; normalized by GAPDH). (E) Immunofluorescence of EGFP and F-actin staining in cells expressing EGFP for control or EGFP-eEF2. Scale, 20 μ m. (F) Quantification shows that the thickness of individual SFs is increased on the overexpression of eEF2 (over-Control, $n = 166$ SFs, 13 cells; over-eEF2, $n = 176$ SFs, 13 cells; from $N = 3$ independent experiments). (G, H) Western blot shows increased expression in NMMIIa and α -actinin-1 on the overexpression of eEF2, but the concomitant change in β -actin is not significant ($N = 3$ independent experiments; normalized by GAPDH). EGFP-eEF2 was detected by the eEF2 antibody.

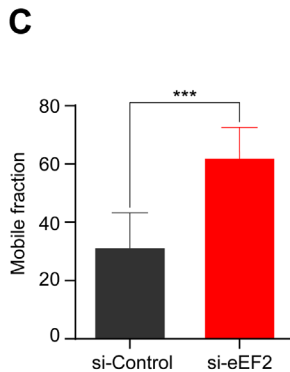
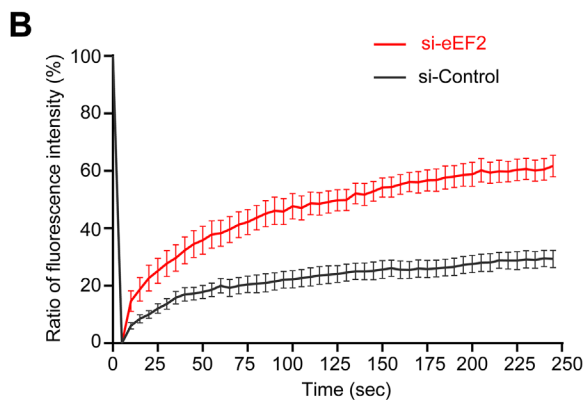
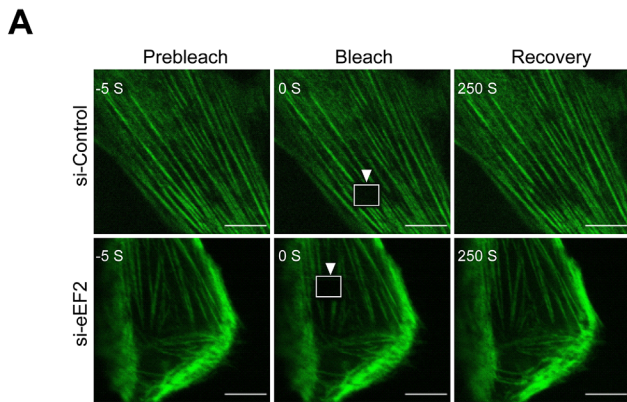


FIGURE 7: eEF2 stabilizes SFs. (A) FRAP experiments were performed on control cells expressing EGFP-MLC and those cells with eEF2 silencing. A rectangular region (indicated by the arrowhead) was bleached at time zero. (B) Time-series change in fluorescence intensity, in which all the values are normalized between the initial and photobleached states and shown in percentage (mean \pm SD; $N = 3$ independent experiments). (C) Quantification of mobile fraction shows that eEF2 silencing results in destabilizing the EGFP-MLC-labeled SFs. Scale, 10 μ m.

LTX Reagent with PLUS Reagent (Thermo Fisher Scientific) or RNAiMAX (Thermo Fisher Scientific), respectively, according to the manufacturer's instructions. For passaging to induce RS, cells were seeded in polystyrene tissue culture flasks at an ~20% density and treated with trypsin at 80–90% confluency; consequently, it took ~80 d in total to obtain P33 cells.

Plasmids and siRNAs

Plasmids encoding human MLC gene combined with EGFP were constructed in our group previously (Huang *et al.*, 2021). The cDNAs encoding human elongation factor eEF2 were amplified by PCR using Q5 High-Fidelity 2X Master Mix (NEB) with primers (forward primer: GCGAAGCTTCGATGGTGAACCTTCACGGT; reverse primer: GCGGCGAATTCCTACAATTTGTCCAGGAAG) and inserted into the pEGFP vector. The siRNAs targeting eEF2 and negative control siRNAs (s4991 and s4492, Thermo Fisher Scientific) were transfected to cells as described above.

Western blotting

Cells were lysed in RIPA buffer (50 mM Tris-HCl, 100 mM NaCl, 1% NP-40, 1% sodium deoxycholate, 1 mM Na₃VO₄, 1 mM NaF, 1 mM dithiothreitol, 1 mM phenylmethylsulfonyl fluoride, 1 μ g/ml pepstatin, and 1 μ g/ml leupeptin; pH 7.4) and centrifuged at 15,000 \times g for 30 min to collect the supernatant. Protein concen-

tration was measured by Pierce BCA Protein Assay Kit (Thermo Fisher Scientific). Proteins were fractionated in 10% gradient acrylamide gels (Bio-Rad). Following SDS-PAGE, samples in gels were transferred onto polyvinylidene fluoride membranes (0.45 μ m, Wako). After blocking in 5% bovine serum albumin for 1 h at room temperature, primary antibodies (Supplemental Table S3) were used and detected using HRP-conjugated anti-rabbit or anti-mouse secondary antibodies (Bio-Rad). The target bands were stained with Immobilon Western Kit (Millipore, Burlington) and analyzed with ImageLab software (Bio-Rad).

Wound healing and proliferation assays

Cell migration was evaluated by performing wound healing assay. The healing rate was quantified 12 h after a linear wounding was made on confluent cells by using a pipette tip. Cell proliferation was evaluated by initially incubating cells with EdU reagent for 36 h and then by staining them using Click-iT EdU Cell Proliferation Kit (Thermo Fisher Scientific).

SA- β -gal staining

Cells cultured on 6-well plates were stained using SA- β -gal activity assay kit (Cell Signaling Technology) according to the manufacturer's instruction. The staining images were taken using a microscope (IX73, Olympus) and analyzed with ImageJ software (National Institutes of Health).

Immunofluorescence

Cells cultured on glass-bottom dishes were fixed with 4% paraformaldehyde in phosphate-buffered saline (Wako) at 37°C for 30 min, permeabilized with 0.1% Triton X-100 for 15 min, blocked with 5% normal goat serum for 1 h, and incubated with the primary antibody (Supplemental Table S3) for 1.5 h and then hybridized with appropriate secondary antibodies (Thermo Fischer Scientific) for 1 h at room temperature. The cell nucleus and actin filaments were stained with Hoechst 33342 (Thermo Fischer Scientific) and fluorescently labeled phalloidin (Thermo Fischer Scientific), respectively. Images were acquired using a microscope (IX73, Olympus) or a confocal laser scanning microscope (FV1000, Olympus) equipped with a UPlan Apo 60 \times oil objective lens (NA = 1.42) and analyzed using ImageJ software.

Isolation of SFs from cells

Cells were cultured to reach ~80% confluency on 60-mm-diameter polystyrene culture dishes. Cells were hypotonically shocked with a low-ionic strength solution (2.5 mM triethanolamine, 1 mM dithiothreitol, 1 μ g/ml pepstatin, and 1 μ g/ml leupeptin in ultrapure water) for 2 min and then were subjected to fluid shearing forces by repeated pipetting in the low-ionic solution for 30 s. The buffer was collected by Centrifugal Filters Kit (Amicon Ultra) to serve as the cell body lysates for Western blot. Ventral SFs remaining bound to the

dish were incubated with 0.05% Triton X-100 in a cytoskeleton stabilizing buffer (20 mM Imidazole, 2.2 mM MgCl₂, 2 mM EGTA, 13.3 mM KCl, 1 mM dithiothreitol, 1 µg/ml pepstatin, and 1 µg/ml leupeptin; pH 7.3; Matsui *et al.*, 2011; Deguchi *et al.*, 2012; Matsui and Deguchi, 2019; Okamoto *et al.*, 2020) for 1 min and then were rinsed 3× with the same buffer free of Triton X-100. The extracted SFs were collected in RIPA buffer on ice.

Quantification of the morphology of SFs

To describe the morphological phenotype of SFs according to fixed criteria, we used the intensity (gray scale) analysis mode in ImageJ software. We determined a representative gray level of the cytoplasmic space by averaging the values of multiple places recognized obviously to be cytoplasmic regions. Among the intracellular structures whose intensity is higher than the representative level of cytoplasmic regions, we regarded a fiberlike structure as SFs except for noisy ones whose peak intensity is much smaller (less than ~30%) than the population of SFs; in addition, short fibers, which cross-link separate SFs, were not counted as SFs in quantifying their number per cell. We took a survey line in a direction perpendicular to each of SFs and then defined and quantified the thickness of individual SFs to be the FWHM, i.e., the distance between the two nearby positions around the edges of a single SF taking an intensity of $[(\text{Peak intensity}) - (\text{Valley intensity})]/2$.

Mass spectrometry-based shotgun proteomics

Cells at P2 and P33 were lysed with nondenatured lysis buffer (50 mM Tris, 2% sodium deoxycholate, 1 mM DTT, 10 µg/ml leupeptin, 10 µg/ml pepstatin, and 1 mM PMSF; pH 8.0). The sample lysates were sequenced by mass spectrometry at the Center for Medical Innovation and Translational Research (COMIT) of Osaka University Medical School using UltiMate 3000 RSLCnano system coupled with Q-Exactive mass spectrometer (Thermo Fisher Scientific) to distinguish between P2 and P33 by identifying protein expression differences. The false discovery rate was set to 1.4% at peptide level. Three independent experiments were carried out to evaluate the reproducibility of the identification. Functional analysis was performed using Scaffold 4 software (Proteome Software).

FRAP

Cells expressing EGFP-MLC were cultured on a glass-bottom dish in a stage incubator (Tokai Hit). FRAP experiments were performed using a confocal microscope (FV1000, Olympus) with a 60× oil immersion objective lens on cells treated in advance with siRNAs for control or for eEF2 for 36 h before the experiments. Photobleaching was induced using the 405/440-nm-wavelength lasers on individual EGFP-MLC-labeled SFs, and images were taken for 4 min at a 5-s interval. The recovery curve was fitted to a single exponential function by the least-squares method, by which the steady-state value of the fluorescence intensity, i.e., mobile fraction, was computed to measure the instability of SFs.

Statistical analysis

Statistical analysis was performed using Prism 8 (GraphPad Software), in which *p* values were calculated using a one-way analysis of variance followed by Tukey's test or two-tailed Student's *t* test for multiple comparisons. Data were shown as mean + SD from more than three independent experiments. Statistical significance was set, compared with respective controls, as follows: **p* < 0.05, ***p* < 0.01, and ****p* < 0.001.

ACKNOWLEDGMENTS

We thank Kazumasa Ohashi for valuable discussions. S.L. and N.K. are supported by a Chinese Scholarship Council (CSC) Scholarship. This work was supported in part by JSPS KAKENHI Grants 18H03518 and 19K22967.

REFERENCES

- Bianco C, Thompson L, Mohr I (2019). Repression of eEF2K transcription by NF-κB tunes translation elongation to inflammation and dsDNA-sensing. *Proc Natl Acad Sci USA* 116, 22583–22590.
- Braga VM, Machesky LM, Hall A, Hotchin NA (1997). The small GTPases Rho and Rac are required for the establishment of cadherin-dependent cell-cell contacts. *J Cell Biol* 137, 1421–1431.
- Burrige K, Wittchen ES (2013). The tension mounts: stress fibers as force-generating mechanotransducers. *J Cell Biol* 200, 9–19.
- Chen CS, Tan J, Tien J (2004). Mechanotransduction at cell-matrix and cell-cell contacts. *Annu Rev Biomed Eng* 6, 275–302.
- Chen QM, Tu VC, Catania J, Burton M, Toussaint O, Dilley T (2000). Involvement of Rb family proteins, focal adhesion proteins and protein synthesis in senescent morphogenesis induced by hydrogen peroxide. *J Cell Sci* 113, 4087–4097.
- Chien S (2007). Mechanotransduction and endothelial cell homeostasis: the wisdom of the cell. *Am J Physiol Heart Circ Physiol* 292, H1209–H1224.
- Choi J, Grosely R, Prabhakar A, Lapointe CP, Wang JF, Puglisi JD (2018). How messenger RNA and nascent chain sequences regulate translation elongation. *Annu Rev Biochem* 87, 421–449.
- Cristofalo VJ, Lorenzini A, Allen RG, Torres C, Tresini M (2004). Replicative senescence: a critical review. *Mech Ageing Dev* 125, 827–848.
- Deguchi S, Matsui TS, Komatsu D, Sato M (2012). Contraction of stress fibers extracted from smooth muscle cells: effects of varying ionic strength. *J Biomech Sci Eng* 7, 388–398.
- Deguchi S, Ohashi T, Sato M (2006). Tensile properties of single stress fibers isolated from cultured vascular smooth muscle cells. *J Biomech* 39, 2603–2610.
- Goldstein S (1990). Replicative senescence: the human fibroblast comes of age. *Science* 249, 1129–1133.
- Gross SR, Kinzy TG (2005). Translation elongation factor 1A is essential for regulation of the actin cytoskeleton and cell morphology. *Nat Struct Mol Biol* 12, 772–778.
- Hamey JJ, Wilkins MR (2018). Methylation of elongation factor 1A: Where, who, and why? *Trends Biochem Sci* 43, 211–223.
- Hayflick L (1965). The limited in vitro lifetime of human diploid cell strains. *Exp Cell Res* 37, 614–636.
- Hirata H, Gupta M, Vedula SR, Lim CT, Ladoux B, Sokabe M (2015). Actomyosin bundles serve as a tension sensor and a platform for ERK activation. *EMBO Rep* 16, 250–257.
- Horvath AI, Gyimesi M, Varkuti BH, Kepiro M, Szegvari G, Lorincz I, Hegyi G, Kovacs M, Malnasi-Csizmadia A (2020). Effect of allosteric inhibition of non-muscle myosin 2 on its intracellular diffusion. *Sci Rep* 10, 13341.
- Hotulainen P, Lappalainen P (2006). Stress fibers are generated by two distinct actin assembly mechanisms in motile cells. *J Cell Biol* 173, 383–394.
- Huang W, Matsui TS, Saito T, Kuragano M, Takahashi M, Kawahara T, Sato M, Deguchi S (2021). Mechanosensitive myosin II but not cofilin primarily contributes to cyclic cell stretch-induced selective disassembly of actin stress fibers. *Am J Physiol Cell Physiol* 320, C1153–C1163.
- Hwang ES, Yoon G, Kang HT (2009). A comparative analysis of the cell biology of senescence and aging. *Cell Mol Life Sci* 66, 2503–2524.
- Jalal S, Shi S, Acharya V, Huang RY, Viasnoff V, Bershadsky AD, Tee YH (2019). Actin cytoskeleton self-organization in single epithelial cells and fibroblasts under isotropic confinement. *J Cell Sci* 132, <https://doi.org/10.1242/jcs.220780>.
- Kang N, Matsui TS, Deguchi S (2021). Statistical profiling reveals correlations between the cell response to and the primary structure of Rho-GAPs. *Cytoskeleton (Hoboken)*.
- Kang N, Matsui TS, Liu S, Fujiwara S, Deguchi S (2020). Comprehensive analysis of the whole Rho-GAP family reveals that ARHGAP4 suppresses EMT in epithelial cells under negative regulation by Septin9. *FASEB J* 34, 8326–8340.
- Katoh K, Kano Y, Masuda M, Onishi H, Fujiwara K (1998). Isolation and contraction of the stress fiber. *Mol Biol Cell* 9, 1919–1938.
- Kaunas R, Deguchi S (2011). Multiple roles for myosin II in tensional homeostasis under mechanical loading. *Cell Mol Bioeng* 4, 182–191.
- Kaunas R, Usami S, Chien S (2006). Regulation of stretch-induced JNK activation by stress fiber orientation. *Cell Signal* 18, 1924–1931.

- Kim S, Coulombe PA (2010). Emerging role for the cytoskeleton as an organizer and regulator of translation. *Nat Rev Mol Cell Biol* 11, 75–81.
- Kreis TE, Birchmeier W (1980). Stress fiber sarcomeres of fibroblasts are contractile. *Cell* 22, 555–561.
- Kumar S, Maxwell IZ, Heisterkamp A, Polte TR, Lele TP, Salanga M, Mazur E, Ingber DE (2006). Viscoelastic retraction of single living stress fibers and its impact on cell shape, cytoskeletal organization, and extracellular matrix mechanics. *Biophys J* 90, 3762–3773.
- Kuo JC, Han X, Hsiao CT, Yates JR 3rd, Waterman CM (2011). Analysis of the myosin-II-responsive focal adhesion proteome reveals a role for beta-Pix in negative regulation of focal adhesion maturation. *Nat Cell Biol* 13, 383–393.
- Levine AJ, Oren M (2009). The first 30 years of p53: growing ever more complex. *Nat Rev Cancer* 9, 749–758.
- Lin YH, Zhen YY, Chien KY, Lee IC, Lin WC, Chen MY, Pai LM (2017). LIMCH1 regulates nonmuscle myosin-II activity and suppresses cell migration. *Mol Biol Cell* 28, 1054–1065.
- Linve A, Geiger B (2016). The inner workings of stress fibers - from contractile machinery to focal adhesions and back. *J Cell Sci* 129, 1293–1304.
- Matsui TS, Deguchi S (2019). Spatially selective myosin regulatory light chain regulation is absent in dedifferentiated vascular smooth muscle cells but is partially induced by fibronectin and Klf4. *Am J Physiol Cell Physiol* 316, C509–C521.
- Matsui TS, Kaunas R, Kanzaki M, Sato M, Deguchi S (2011). Non-muscle myosin II induces disassembly of actin stress fibres independently of myosin light chain dephosphorylation. *Interface Focus* 1, 754–766.
- McHugh D, Gil J (2018). Senescence and aging: Causes, consequences, and therapeutic avenues. *J Cell Biol* 217, 65–77.
- Meng W, Takeichi M (2009). Adherens junction: molecular architecture and regulation. *Cold Spring Harb Perspect Biol* 1, a002899.
- Muller M (2009). Cellular senescence: molecular mechanisms, in vivo significance, and redox considerations. *Antioxid Redox Signal* 11, 59–98.
- Nishio K, Inoue A (2005). Senescence-associated alterations of cytoskeleton: extraordinary production of vimentin that anchors cytoplasmic p53 in senescent human fibroblasts. *Histochem Cell Biol* 123, 263–273.
- Oji Y, Tatsumi N, Fukuda M, Nakatsuka S, Aoyagi S, Hirata E, Nanchi I, Fujiki F, Nakajima H, Yamamoto Y, et al. (2014). The translation elongation factor eEF2 is a novel tumor-associated antigen overexpressed in various types of cancers. *Int J Oncol* 44, 1461–1469.
- Okamoto T, Matsui TS, Ohishi T, Deguchi S (2020). Helical structure of actin stress fibers and its possible contribution to inducing their direction-selective disassembly on cell shortening. *Biomech Model Mechanobiol* 19, 543–555.
- Rong F, Liu L, Zou C, Zeng J, Xu YS (2020). MALAT1 promotes cell tumorigenicity through regulating miR-515-5p/EEF2 axis in non-small cell lung cancer. *Cancer Manag Res* 12, 7691–7701.
- Saito T, Huang W, Matsui TS, Kuragano M, Takahashi M, Deguchi S (2021). What factors determine the number of nonmuscle myosin II in the sarcomeric unit of stress fibers? *Biomech Model Mechanobiol* 20, 155–166.
- Silva RC, Sattlegger E, Castilho BA (2016). Perturbations in actin dynamics reconfigure protein complexes that modulate GCN2 activity and promote an eIF2 response. *J Cell Sci* 129, 4521–4533.
- Simpson LJ, Reader JS, Tzima E (2020). Mechanical forces and their effect on the ribosome and protein translation machinery. *Cells* 9, <https://doi.org/10.3390/cells9030650>.
- Sun W, Wei X, Niu A, Ma X, Li JJ, Gao D (2015). Enhanced anti-colon cancer immune responses with modified eEF2-derived peptides. *Cancer Lett* 369, 112–123.
- Tojkander S, Gateva G, Schevzov G, Hotulainen P, Naumanen P, Martin C, Gunning PW, Lappalainen P (2011). A molecular pathway for myosin II recruitment to stress fibers. *Curr Biol* 21, P539–P550.
- Tojkander S, Gateva G, Lappalainen P (2012). Actin stress fibers—assembly, dynamics and biological roles. *J Cell Sci* 125, 1855–1864.
- van Deursen JM (2014). The role of senescent cells in ageing. *Nature* 509, 439–446.
- Verpelli C, Piccoli G, Zanchi A, Gardoni F, Huang K, Brambilla D, Di Luca M, Battaglioli E, Sala C (2010). Synaptic activity controls dendritic spine morphology by modulating eEF2-dependent BDNF synthesis. *J Neurosci* 30, 5830–5842.
- Watanabe T, Hosoya H, Yonemura S (2007). Regulation of myosin II dynamics by phosphorylation and dephosphorylation of its light chain in epithelial cells. *Mol Biol Cell* 18, 605–616.
- Wei F, Xu X, Zhang C, Liao Y, Ji B, Wang N (2020). Stress fiber anisotropy contributes to force-mode dependent chromatin stretching and gene upregulation in living cells. *Nat Commun* 11, 4902.